


Voxel-based whole-lesion enhancement parameters: a study of its clinical value in differentiating clear cell renal cell carcinoma from renal oncocytoma

Frank Chen , Mittul Gulati, Darryl Hwang, Steven Cen, Felix Yap, Chidubem Ugwueze, Bino Varghese, Mihir Desai, Manju Aron, Inderbir Gill, Vinay Duddalwar

Keck School of Medicine, University of Southern California, 1500 San Pablo St, 2nd Floor Imaging, Los Angeles, CA 90033, USA

Abstract

Purpose: The purpose of this study was to compare whole-lesion (WL) enhancement parameters to single region of interest (ROI)-based enhancement in discriminating clear cell renal cell carcinoma (ccRCC) from renal oncocytoma.

Materials and Methods: In this IRB-approved retrospective study, the surgical database was queried to derive a cohort of 94 postnephrectomy patients with ccRCC or oncocytoma (68 ccRCC, 26 oncocytoma), who underwent preoperative multiphase contrast-enhanced computed tomography (CECT) between June 2009 and August 2013. CT acquisitions were transferred to a three-dimensional workstation, and WL ROIs were manually segmented. WL enhancement and histogram distribution parameters skewness, kurtosis, standard deviation (SD), and interquartile range (IQR) were calculated. WL enhancement parameters were compared to single ROI-based enhancement using receiver operating characteristic (ROC) analysis.

Results: Oncocytoma had significantly higher WL enhancement than ccRCC in nephrographic (mean, $p = 0.02$; median, $p = 0.03$) and excretory phases (mean, $p = 0.03$; median $p < 0.01$). ccRCC had significantly higher kurtosis than oncocytoma in corticomedullary ($p = 0.03$) and excretory phases ($p < 0.01$), and significantly higher SD and IQR than oncocytoma in all postcontrast phases: corticomedullary (SD, $p = 0.02$; IQR, $p < 0.01$), nephrographic (SD, $p = 0.01$; IQR, $p = 0.03$), and excretory (SD, $p < 0.01$; IQR, $p < 0.01$). When compared to single ROI-based

enhancement, WL enhancement alone did not demonstrate a statistical advantage in discriminating between ccRCC and oncocytoma (area under ROC curve of 0.78 and 0.72 respectively), but when combined with histogram distribution parameters (area under ROC curve of 0.86), it did demonstrate a slight improvement.

Conclusion: Our study suggests that voxel-based WL enhancement parameters provide only a slight improvement over single ROI-based enhancement techniques in differentiating between ccRCC and renal oncocytoma.

Key words: Clear cell renal cell carcinoma—Oncocytoma—CT—Whole-lesion enhancement—Histogram distribution

Clear cell renal cell carcinoma (ccRCC) is the most common subtype of renal cell carcinoma, accounting for 60–65% of renal cell cancers [1]. ccRCC has a greater propensity for vascular invasion and a greater likelihood to metastasize at an early stage than do other renal cell carcinoma subtypes [2]. Renal oncocytoma is the most common benign solid renal neoplasm, accounting for 3–7% of all adult renal epithelial neoplasms [3]. Unlike ccRCC, oncocytoma has an excellent prognosis with a benign natural history, except for very rare instances of distant metastases and hybrid tumors with renal cell carcinoma [4].

Despite its excellent prognosis and benign natural history, oncocytoma is commonly treated by surgical resection due to the inability to confidently differentiate it from ccRCC in the preoperative setting. This includes difficulty in conclusively classifying it on either preoperative imaging or biopsy. Numerous studies have

attempted to distinguish oncocytoma from ccRCC on multiphase, multidetector computed tomography using both qualitative and quantitative measures. The classic imaging appearance of oncocytoma is a well-demarcated, homogeneous enhancing mass with a central stellate scar and a lack of hemorrhage, necrosis, calcification, and macroscopic fat [5–8]. However, these classic imaging features are only seen in a minority of cases and are not entirely specific to oncocytoma [9]. Segmental enhancement inversion has been described as a characteristic enhancement pattern of oncocytoma. It is seen in oncocytoma which has two distinct areas demonstrating different degrees of enhancement. The more hyperattenuating area on corticomedullary phase becomes more hypoattenuating on excretory phase, whereas the more hypoattenuating area on corticomedullary phase becomes more hyperattenuating on excretory phase [10]. However, proposing segmental enhancement inversion as a characteristic enhancement pattern of oncocytoma has been controversial [11–13].

Quantitative methods of differentiating oncocytoma from ccRCC have relied on the placement of regions of interest (ROI) on renal tumors to evaluate tumor enhancement characteristics. The ROI is often subcentimeter in size and is typically placed on what is deemed the most avidly enhancing portion of the tumor. This method is limited by sampling errors and interobserver variability in ROI placement [14–22]. Whole-lesion analysis of renal tumors would resolve these limitations.

The purpose of our study is to evaluate the use of voxel-based whole-lesion enhancement parameters on contrast-enhanced CT (CECT) to distinguish oncocytoma from ccRCC.

Materials and methods

Patients

This study was institutional review board (IRB)-approved and Health Insurance Portability and Accountability Act-compliant. Patients were identified by retrospectively querying our prospectively maintained surgical database for all post nephrectomy patients who had pathology-proven oncocytoma or ccRCC and who had preoperative multiphase CECT of the abdomen between June 2009 and August 2013. Pathologic evaluation was performed by specialized genitourinary pathologists, and histologic subtype was defined according to the World Health Organization 2004 classification [23].

CT examination

All CT examinations were performed with a 64-detector row helical CT scanner (Brilliance, Philips Healthcare, CT). The CT scans were obtained during patient breath-holding with the following parameters: 120 kVp, variable tube current, slice thickness of 0.5 mm with reconstruc-

tion interval of 2 mm. Noncontrast, corticomedullary, nephrographic, and excretory phase images of the abdomen were obtained. The pelvis was included on the nephrographic phase images. Approximately 100–150 mL of nonionic intravenous contrast material (Isovue 350; Bracco Imaging) dosed to weight was administered with a power injector at a rate of 4–5 mL/s. Fixed time delay to scanning for corticomedullary phase images, nephrographic phase images, and excretory phase images were 25, 90 s, and 5 min postcontrast injection, respectively.

CT analysis

Multiphase CT acquisitions were transferred to our dedicated three-dimensional workstation (Synapse 3D; Fujifilm Medical Systems, Stamford, CT). Renal tumors were manually segmented in Synapse 3D as 3D ROIs. Tumor segmentation was performed by a third year medical student (C.U.) and a second year radiology resident (F.Y.), and reviewed by an abdominal fellowship-trained radiologist with 15 years' experience for accuracy. All three individuals involved in tumor segmentation were blinded to clinical and pathologic information. The kidney and tumor were segmented out in all phases to facilitate co-registration. The DICOM-formatted CT images were converted into NIfTI-1 volumes. DICOM keeps the images as individual slices, while NIfTI-1 treats images as multidimensional volumes. The series of images were then co-registered using normalized mutual information cost function implemented in the Statistical Parametric Mapping software package. The custom MATLAB code was used to extract voxel data corresponding to the ROI. Contrast-enhanced absolute voxel enhancement values were displayed as a histogram. The histogram distribution parameters were computed using custom MATLAB analysis framework. The mean and median absolute enhancement and histogram distribution parameters skewness, kurtosis, standard deviation, and interquartile range were computed for each lesion on all phases.

Subsequently, two abdominal fellowship-trained radiologists with 5 years (F.K.C) and 4 years of experience (M.G.), who were blinded to clinical and pathologic information, independently reviewed all multiphase CT examinations. They placed a single ROI of approximately 0.5 cm² on the most avidly enhancing portion of heterogeneously enhancing renal tumors in the corticomedullary phase and on the approximate same region of the tumor in the nephrographic and delayed phases. Single ROI was placed in the center of homogeneously enhancing lesions in corticomedullary, nephrographic, and delayed phases. Mean and median absolute enhancement of ccRCC and renal oncocytoma were calculated based on single ROI-based enhancement technique.

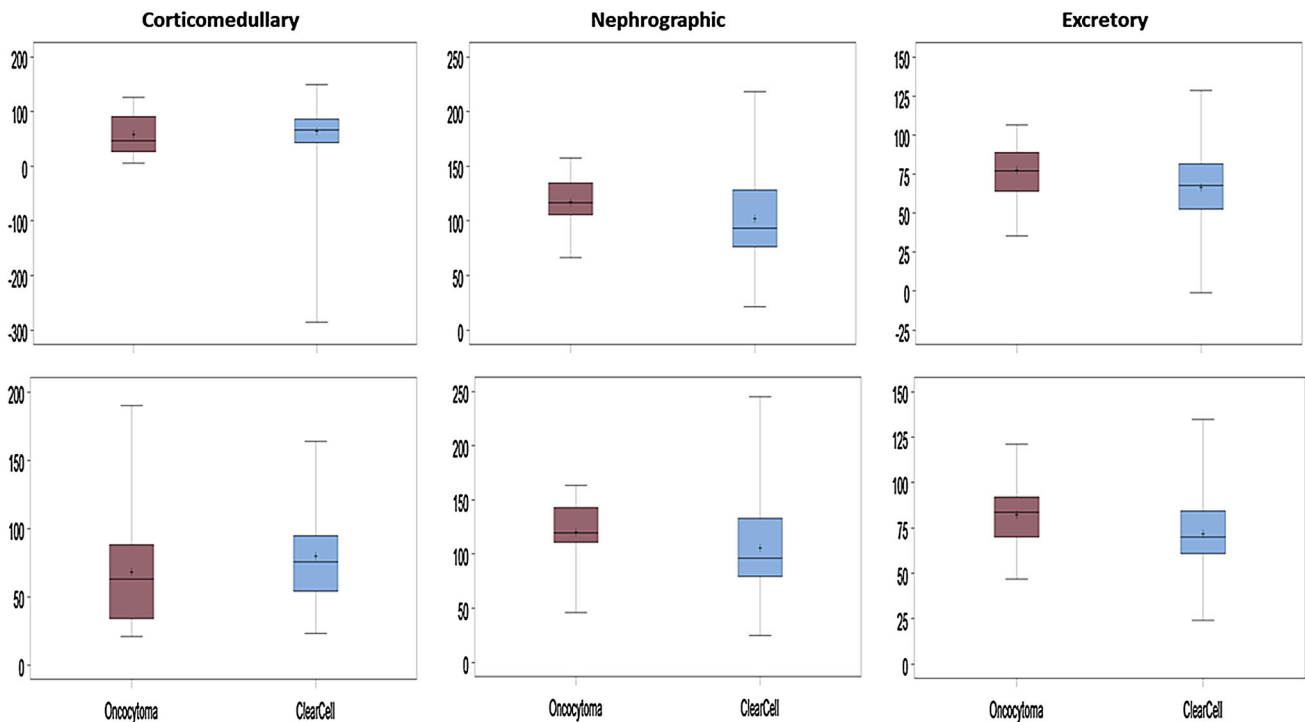


Fig. 1. Box plot of mean (*top row*) and median (*bottom row*) whole-lesion enhancement.

Statistical analysis

The data distribution was examined using D'Agostino's K-squared test and histogram-based visual inspection. For a normally distributed variable, the independent t test was used to explore the difference between ccRCC and oncocytoma. If not normally distributed, the Wilcoxon rank sum test was used. P values less than 0.05 were considered to indicate statistical significance. The Receiver Operating Characteristic (ROC) curves were used to assess the prediction accuracy. The area under the curve (AUC) was used to compare the discrimination power between the different imaging quantitative methods. For the parameters derived from histogram analysis, the final predictors were selected using stepwise logistic regression with backward selection.

Results

Patients

Between June 2009 and August 2013, a total of 113 postnephrectomy patients who had preoperative multiphase CECT performed at our institution were found to have pathology-proven oncocytoma or renal cell carcinoma. Among the 113 patients, 68 patients had ccRCC, 15 patients had papillary renal cell carcinoma, 4 patients had chromophobe renal cell carcinoma, and 26 patients had oncocytoma. Given the relatively lower number of papillary and chromophobe renal cell carcinomas com-

pared to ccRCC and oncocytoma, a decision was made to only compare ccRCC and oncocytoma in this study. Of the 94 patients included in the study, 67 (71%) were male, and 27 (29%) were female. The mean age of patients with ccRCC was 62 years (range 31–82 years), and the mean age of patients with oncocytoma was 67 years (range 48–86 years). The mean tumor diameter was 4.5 cm for ccRCC (range 0.7–10.0 cm) and 4.9 cm for oncocytoma (range 1.2–11.0 cm).

Single ROI-based enhancement

The single ROI-based enhancement of ccRCC was significantly higher than that of oncocytoma in the corticomedullary phase (155 HU vs. 116 HU, $p = 0.03$). The single ROI-based enhancement of oncocytoma was higher than that of ccRCC in nephrographic and excretory phases, but this was not statistically significant (nephrographic, 139 HU vs. 128 HU, $p = 0.21$; excretory, 82 HU vs. 75 HU, $p = 0.12$). The ROC curve based on single ROI-based enhancement had an AUC of 0.78 with 95% confidence limits of 0.66–0.89 (Fig. 2).

Whole-lesion enhancement

The mean and median whole-lesion enhancement of oncocytoma and ccRCC are summarized in Table 1 with box plot in Fig. 1. There was no significant difference between the mean and median precontrast density of

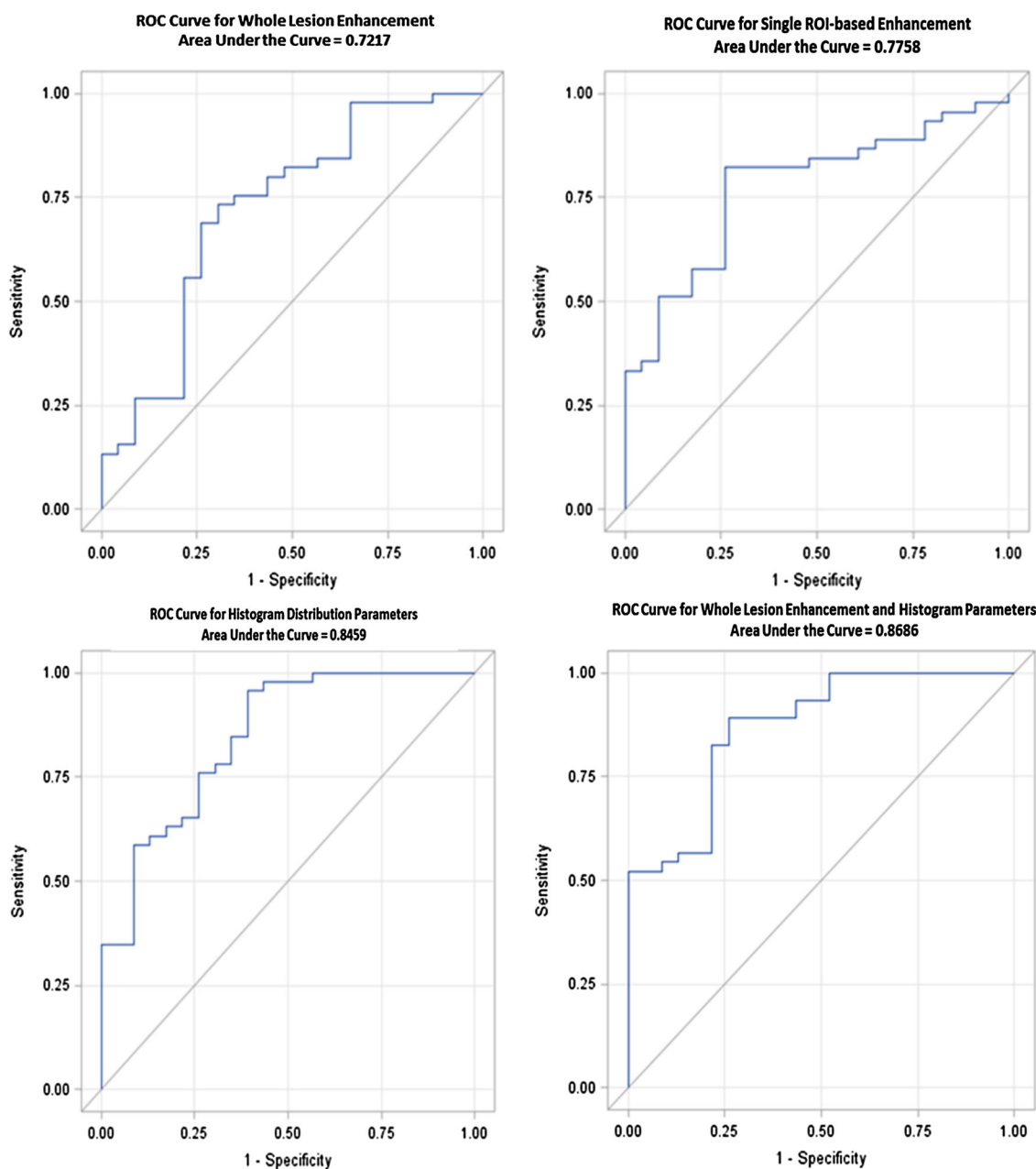


Fig. 2. ROC curves.

ccRCC and oncocytoma (mean density, 3 HU vs. 9 HU, $p = 0.97$; median density, 23 HU vs. 15 HU, $p = 0.33$). The mean and median enhancement of oncocytoma were significantly higher than that of ccRCC in the nephrographic phase (mean enhancement, 117 HU vs. 102 HU, $p = 0.02$; median enhancement, 120 HU vs. 106 HU, $p = 0.03$) and excretory phase (mean enhancement, 78 HU vs. 67 HU, $p = 0.03$; median enhancement, 82 HU vs. 72 HU, $p < 0.01$) (Figs. 3, 4). The mean and median enhancement of ccRCC were higher than oncocytoma on corticomedullary phase, but this was not statistically significant (mean enhancement, 64 HU vs. 58 HU, $p = 0.17$; median enhancement, 80 HU vs. 68 HU,

$p = 0.1$). The mean and median deenhancement of oncocytoma from nephrographic phase to excretory phase (absolute enhancement on nephrographic phase minus absolute enhancement on excretory phase) were higher than that of ccRCC, but this was not statistically significant (mean deenhancement, 39 HU vs. 36 HU, $p = 0.29$; median deenhancement, 39 HU vs. 35 HU, $p = 0.12$). The ROC curve based on whole-lesion enhancement had an AUC of 0.72 with 95% confidence limits of 0.58–0.86 (Fig. 2). The difference in AUC between single ROI enhancement and whole-lesion enhancement was -0.05 (95% CI -0.16 to 0.06 ; $p = 0.35$).

Table 1. Whole-lesion enhancement of ccRCC and oncocytoma

Enhancement	ccRCC	Oncocytoma	<i>p</i> value
CMP-Mean	64.07 ± 57.49	57.7 ± 36.53	0.17
CMP-Median	79.93 ± 36.14	68.08 ± 41.24	0.1
NP-Mean	101.93 ± 35.69	116.92 ± 24.75	0.02*
NP-Median	105.8 ± 38.87	120 ± 28.47	0.03*
EP-Mean	66.54 ± 24.73	77.56 ± 18.7	0.03*
EP-Median	71.64 ± 19.93	82.4 ± 16.09	<0.01*

CMP, corticomedullary phase; NP, nephrographic phase; EP, excretory phase; ccRCC, clear cell renal cell carcinoma

* Statistically significant

Table 2. Histogram distribution parameters of ccRCC and oncocytoma

Histogram distribution parameter	ccRCC (Hounsfield units)	Oncocytoma (Hounsfield units)	<i>p</i> value
CMP-SD	88.74 ± 73.85	59.77 ± 40.92	0.02*
CMP-IQR	854.69 ± 482.2	443.88 ± 325.5	<0.01*
CMP-Kurtosis	25.97 ± 38.23	7.46 ± 18.48	0.03*
CMP-Skewness	-2.77 ± 2.91	-1.45 ± 1.66	0.2
NP-SD	49.67 ± 11.98	43.31 ± 7.36	0.01*
NP-IQR	405.93 ± 105.2	363.19 ± 60.21	0.03*
NP-Kurtosis	2.18 ± 5.39	2.02 ± 1.6	0.15
NP-Skewness	-0.48 ± 0.85	-0.73 ± 0.64	0.08
EP-SD	71.14 ± 48.74	41.35 ± 18.26	<0.01*
EP-IQR	1050 ± 598	518.35 ± 460	<0.01*
EP-Kurtosis	56.07 ± 62.76	31.62 ± 65.46	<0.01*
EP-Skewness	-2.04 ± 5.26	-1.82 ± 3.96	0.85

CMP, corticomedullary phase; NP, nephrographic phase; EP, excretory phase; SD, standard deviation; IQR, interquartile range; ccRCC, clear cell renal cell carcinoma

* Statistically significant

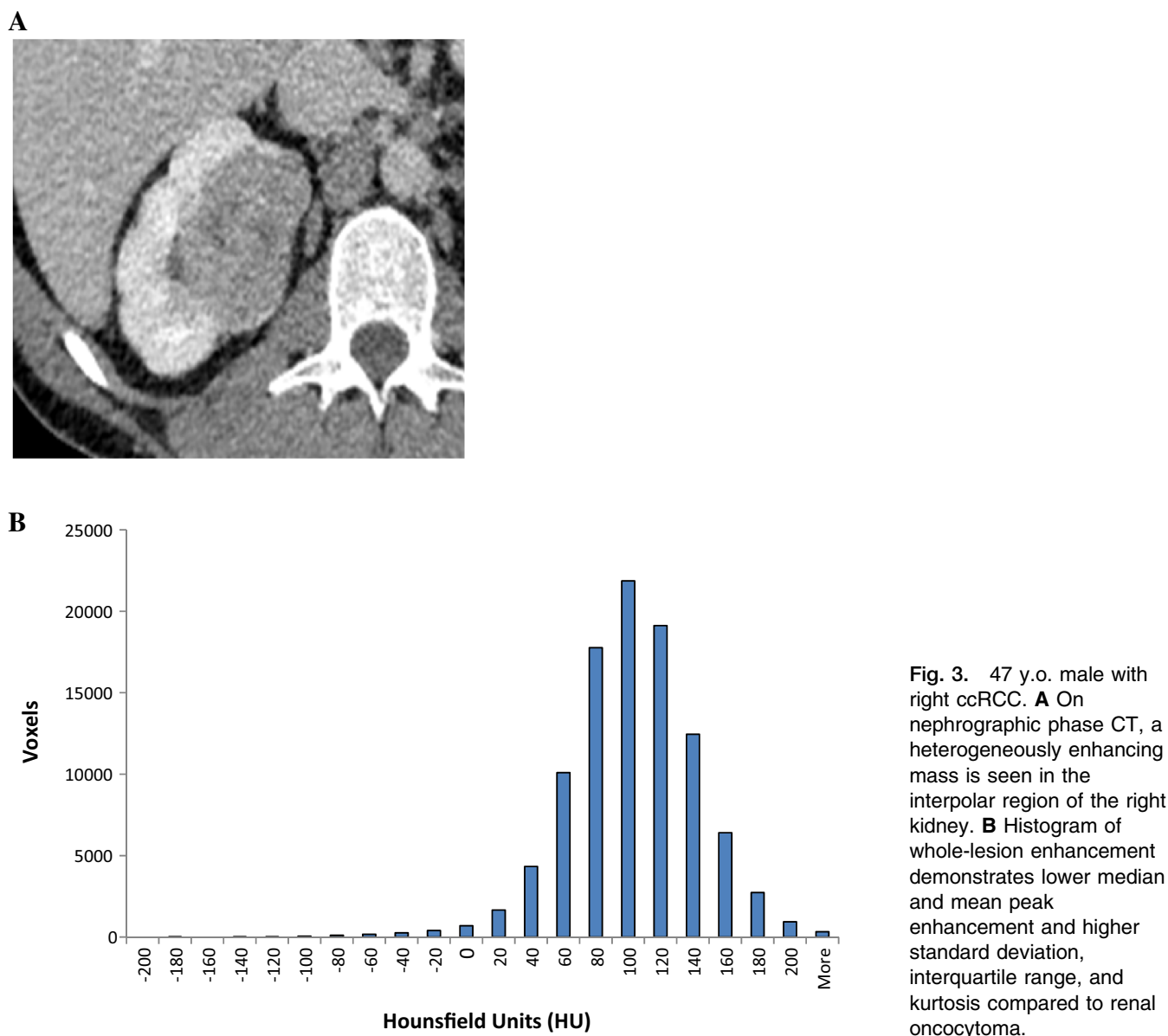
Histogram distribution parameters

The histogram distribution parameters skewness, kurtosis, standard deviation, and interquartile range of oncocytoma and ccRCC are summarized in Table 2. The standard deviation and interquartile range of ccRCC were significantly higher than those of oncocytoma in all postcontrast phases, they were as follows: corticomedullary phase (standard deviation, 89 vs. 60, $p = 0.02$; interquartile range, 855 vs. 444, $p < 0.01$), nephrographic phase (standard deviation, 50 vs. 43, $p = 0.01$; interquartile range, 406 vs. 363, $p = 0.03$), and excretory phase (standard deviation, 71 vs. 41, $p < 0.01$; interquartile range, 1050 vs. 518, $p < 0.01$) (Figs. 3, 4). The kurtosis of ccRCC was significantly higher than that of oncocytoma in the corticomedullary (kurtosis, 26 vs. 7, $p = 0.03$) and excretory phases (kurtosis, 56 vs. 32, $p < 0.01$). In the nephrographic phase, kurtosis of ccRCC was higher than that of oncocytoma, but this was not significantly higher (kurtosis, 2.2 vs. 2.0, $p = 0.15$). There were no significant differences in skewness between oncocytoma and ccRCC on any phases. The ROC curve based on histogram distribution parameters, including corticomedullary phase interquartile range, excretory phase skewness, nephrographic phase standard deviation, and excretory phase interquartile range, had an AUC of 0.85 with 95% confidence limits of 0.75–0.95. When histogram distribution parameters were added to whole-lesion enhancement, the AUC changed from 0.72 (95% CI 0.58–0.86) to

0.86 (95% CI 0.75–0.94) with a slight improvement of 0.14 (95% CI 0.03–0.25; $p = 0.01$) (Fig. 2).

Discussion

It is important to distinguish between oncocytoma and ccRCC because of the differences in prognosis and tumor behavior. Despite their differences in prognosis and tumor behavior, the initial treatment of both neoplasms is often the same given the difficulty in accurately diagnosing them in the preoperative setting. According to the American Urological Association, if technically feasible, the standard of care for the treatment of clinical T1 renal mass is partial nephrectomy. If partial nephrectomy is not technically feasible, radical nephrectomy is the alternate standard of care. For patients at high surgical risk due to major comorbidities or for those who do not wish to undergo surgery, ablative techniques and active surveillance are additional options [24]. Small renal masses measuring less than 3 cm have recently been shown to have a slow growth rate and low metastatic potential, suggesting that active surveillance may be an acceptable initial treatment of these lesions [25–31]. If oncocytoma can be reliably differentiated from ccRCC and other renal malignancies, active surveillance may also be an acceptable initial treatment approach for this benign neoplasm. One method to differentiate oncocytoma from ccRCC is percutaneous biopsy. However, currently, the use of percutaneous biopsy of renal masses is limited given the risks of false negative results, and the



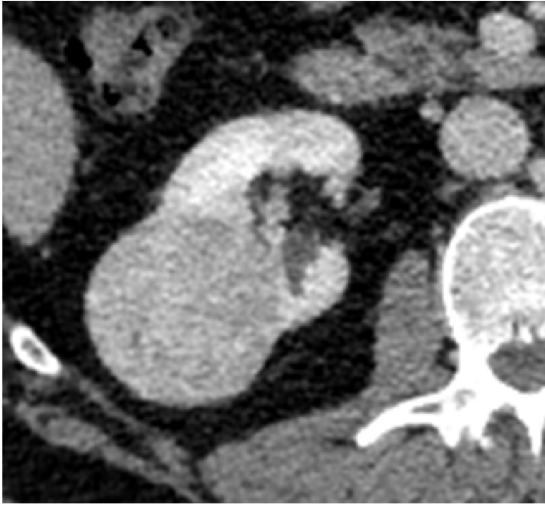
difficulty to consistently discriminate between renal cell carcinoma and oncocytoma on pathology [32–36]. CECT or MRI would be less invasive techniques to differentiate oncocytoma from ccRCC.

On CECT, quantitative studies comparing oncocytoma and ccRCC have provided mixed and sometimes contradictory results. Bird et al. described that oncocytoma demonstrated greater enhancement than ccRCC on arterial, venous, and delayed phases with both tumors having peak enhancement during arterial phase [16]. Young et al. and Gakis et al. described that ccRCC demonstrated greater enhancement than oncocytoma on corticomedullary, nephrographic, and excretory phases with both tumors having peak enhancement during corticomedullary phase [20, 21]. Zhang et al. described that oncocytoma demonstrated greater enhancement than ccRCC on parenchymal and delayed phases with

peak enhancement of both tumors during parenchymal phase [19]. Pierorazio et al. described that oncocytoma demonstrated peak enhancement during nephrographic phase, while ccRCC demonstrated peak enhancement during corticomedullary phase [17]. Quantitative studies of oncocytoma and ccRCC are based on placement of ROI, often subcentimeter in size, on the portion of tumor deemed most avidly enhancing. This method of tumor analysis is hindered by interobserver variability and sampling errors, which may partly explain the contradictory results of the above studies.

In our study, we sought to determine whether voxel-based whole-lesion enhancement parameters on CECT can be used to discriminate between oncocytoma and ccRCC. Whole-lesion evaluation eliminates interobserver variability and sampling errors that limit ROI-based evaluation of renal tumors. We found that the

A



B

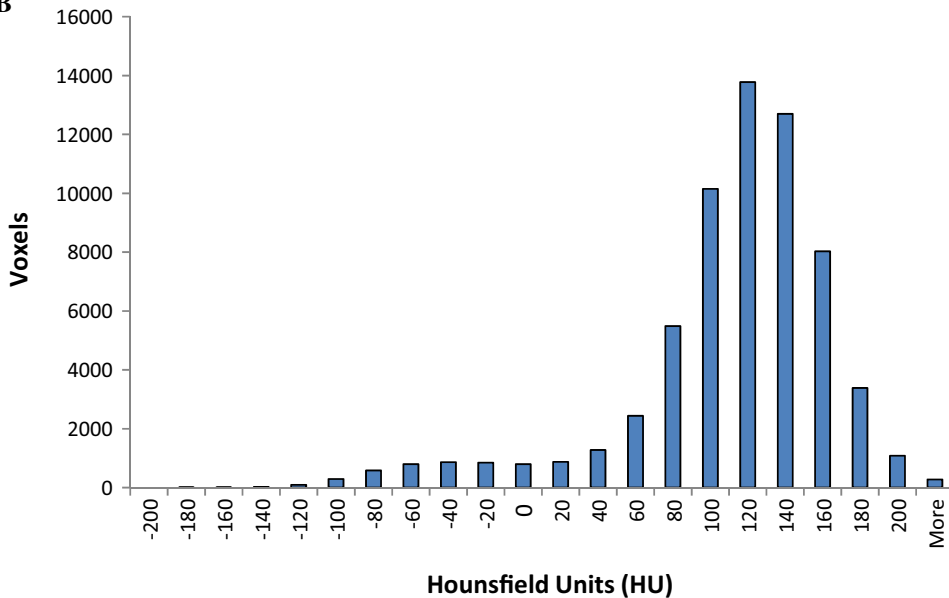


Fig. 4. 59 y.o. male with right renal oncocytoma. **A** On nephrographic phase CT, a homogeneously enhancing mass is seen in the interpolar region of the right kidney. **B** Histogram of whole-lesion enhancement demonstrates higher median and mean peak enhancement and lower standard deviation, interquartile range, and kurtosis compared to ccRCC.

mean and median whole-lesion enhancement of oncocytoma were significantly higher than that of ccRCC on nephrographic and excretory phases. On corticomedullary phase, mean and median whole-lesion enhancement of oncocytoma were also higher than that of ccRCC, but this was not statistically significant. Both tumors demonstrated peak mean and median enhancement on nephrographic phase. Mean and median whole-lesion deenhancement of oncocytoma from nephrographic phase to excretory phase were not significantly different than that of ccRCC. When compared to single ROI-based enhancement, whole-lesion enhancement did not demonstrate a statistical difference in discriminating between ccRCC and oncocytoma.

In our study, we also compared the histogram distribution parameters kurtosis, skewness, standard devi-

ation, and interquartile range of oncocytoma and ccRCC. Kurtosis measures the peakedness of a distribution. A distribution with high kurtosis tends to have a distinct peak which then rapidly declines around this peak. A distribution with low kurtosis is more uniform and tends to have a more flattened peak with more gradual declination around it. Skewness measures the degree of asymmetry in a distribution. The skewness of a normal distribution is zero. All four histogram distribution parameters are ways to evaluate variance within a dataset. On CECT and MRI, ccRCC is considered to be more heterogeneous than oncocytoma, and its voxel-based whole-lesion dataset would be expected to have greater variance than the voxel-based whole-lesion dataset of oncocytoma. As expected, in our study, ccRCC had higher kurtosis, standard deviation, and

interquartile range than oncocytoma on all postcontrast phases. They were all statistically significant except for kurtosis on nephrographic phase. The skewness of ccRCC was not significantly different than that of oncocytoma on all postcontrast phases. When histogram distribution parameters were combined with whole-lesion enhancement, they did demonstrate a slight improvement in discriminating between ccRCC and oncocytoma when compared to single ROI-based enhancement alone. To the best of our knowledge, our study is the first to evaluate the use of whole-lesion histogram distribution parameters to distinguish oncocytoma from ccRCC. Other studies have evaluated the use of whole-lesion histogram distribution parameters to distinguish ccRCC from papillary renal cell carcinoma and to distinguish lipid poor angiomyolipoma from renal cell carcinoma [37–39].

Our study has a few potential limitations. First, our study was a single-center retrospective study. Second, we did not compare oncocytoma with other subtypes of renal cell carcinoma, which have a lower incidence than ccRCC. The data presented and parameters herein developed need to be validated by prospective and/or multicenter studies with consideration toward including additional subtypes of renal cell carcinoma. Third, whole-lesion evaluation of renal tumors is more technically challenging and time consuming than both qualitative assessment and single ROI-based evaluation of renal tumors, and may not be feasible for all clinical settings. In order for whole-lesion evaluation to be feasible in all clinical settings, software needs to be created, which would automate whole-lesion segmentation, simplifying whole-lesion evaluation.

In conclusion, our study demonstrates that whole-lesion enhancement does not provide a statistical advantage over single ROI-based enhancement in differentiating between ccRCC and renal oncocytoma. When whole-lesion enhancement is combined with histogram distribution parameters, there is only a slight improvement over single ROI-based enhancement in differentiating between these two renal tumors. This slight improvement probably does not justify the use of voxel-based whole-lesion enhancement parameters in differentiating between ccRCC and renal oncocytoma in everyday clinical practice, given the expertise and time needed to apply this technique.

Compliance with Ethical Standards

Funding This project has received funding from the Whittier foundation. The project described was supported in part by the Award Number P30CA014089 from the National Cancer Institute. The content is solely the responsibility of the authors and does not necessarily represent the official views of the National Cancer Institute or the National Institutes of Health.

Conflict of Interest None of the authors have any conflict of interest to disclose.

Ethical Approval All procedures performed in studies involving human participants were in accordance with the ethical standards of the institutional and/or national research committee, and with the 1964 Helsinki declaration and its later amendments or comparable ethical standards.

References

1. Reuter VE (2006) The pathology of renal epithelial neoplasms. *Semin Oncol* 33(5):534–543
2. Mai KT, Landry DC, Robertson SJ, et al. (2001) A comparative study of metastatic renal cell carcinoma with correlation to subtype and primary tumor. *Pathol Res Pract* 197(10):671–675
3. Trpkov K, Yilmaz A, Uzer D, et al. (2010) Renal oncocytoma revisited: a clinicopathological study of 109 cases with emphasis on problematic diagnostic features. *Histopathology* 57(6):893–906
4. Schatz SM, Lieber MM (2003) Update on oncocytoma. *Curr Urol Rep* 4(1):30–35
5. Jasinski RW, Amendola MA, Glazer GM, Bree RL, Gikas PW (1985) Computed tomography of renal oncocytomas. *Comput Radiol* 9:307–314
6. Tikkakoski T, Paivansalo M, Alanen A, et al. (1991) Radiologic findings in renal oncocytoma. *Acta Radiol* 32:363–367
7. Quinn MJ, Hartman DS, Friedman AC, et al. (1994) Renal oncocytoma: new observations. *Radiology* 153:49–53
8. Levine E, Huntrakoon M (1983) Computed tomography of renal oncocytoma. *Am J Roentgenol* 141(4):741–746
9. Prasad SR, Surabhi VR, Menias CO, Raut AA, Chintapalli KN (2008) Benign renal neoplasms in adults: cross-sectional imaging findings. *Am J Roentgenol* 190(1):158–164
10. Kim JI, Cho JY, Moon KC, Lee HJ, Kim SH (2009) Segmental enhancement inversion at biphasic multidetector CT: characteristic finding of small renal oncocytoma. *Radiology* 252(2):441–448
11. Schieda N, McInnes MD, Cao L (2014) Diagnostic accuracy of segmental enhancement inversion for diagnosis of renal oncocytoma at biphasic contrast enhanced CT: systematic review. *Eur Radiol* 24(6):1421–1429
12. O'Malley ME, Tran P, Hanbidge A, Rogalla P (2012) Small renal oncocytomas: is segmental enhancement inversion a characteristic finding at biphasic MDCT? *Am J Roentgenol* 199(6):1312–1315
13. McGahan JP, Lamba R, Fisher J, et al. (2011) Is segmental enhancement inversion on enhanced biphasic MDCT a reliable sign for the noninvasive diagnosis of renal oncocytomas? *Am J Roentgenol* 197(4):W674–W679
14. Ishigami K, Jones AR, Dahmouh L, et al. (2015) Imaging spectrum of renal oncocytomas: a pictorial review with pathologic correlation. *Insights Imaging* 6(1):53–64
15. Choudhary S, Rajesh A, Mayer NJ, Mulcahy KA, Haroon A (2009) Renal oncocytoma: CT features cannot reliably distinguish oncocytoma from other renal neoplasms. *Clin Radiol* 64(5):517–522
16. Bird VG, Kanagarajah P, Morillo G, et al. (2011) Differentiation of oncocytoma and renal cell carcinoma in small renal masses (<4 cm): the role of 4-phase computerized tomography. *World J Urol* 29(6):787–792
17. Pierorazio PM, Hyams ES, Tsai S, et al. (2013) Multiphasic enhancement patterns of small renal masses (≤ 4 cm) on preoperative computed tomography: utility for distinguishing subtypes of renal cell carcinoma, angiomyolipoma, and oncocytoma. *Urology* 81(6):1265–1271
18. Millet I, Doyon FC, Hoa D, et al. (2011) Characterization of small solid renal lesions: can benign and malignant tumors be differentiated with CT? *Am J Roentgenol* 197(4):887–896
19. Zhang J, Lefkowitz RA, Ishill NM, et al. (2007) Solid renal cortical tumors: differentiation with CT. *Radiology* 244(2):494–504
20. Gakis G, Kramer U, Schilling D, et al. (2011) Small renal oncocytomas: differentiation with multiphase CT. *Eur J Radiol* 80(2):274–278
21. Young JR, Margolis D, Sauk S, et al. (2013) Clear cell renal cell carcinoma: discrimination from other renal cell carcinoma subtypes and oncocytoma at multiphasic multidetector CT. *Radiology* 267(2):444–453
22. Lee-Felker SA, Felker ER, Tan N, et al. (2014) Qualitative and quantitative MDCT features for differentiating clear cell renal cell

- carcinoma from other solid renal cortical masses. *Am J Roentgenol* 203:W516–W524
23. Eble J, Sauter G, Epstein J (2004) *World Health Organization classification of tumours: pathology and genetics of tumours of the urinary system and male genital organs*. Lyon: IARC Press
 24. Algorithm of Clinical Management of Clinical T1 Renal Mass. 2009. <https://www.auanet.org/common/pdf/education/clinical-guidance/Renal-Mass-Algorithm.pdf>. Accessed 27 Oct 2015.
 25. Thompson RH, Hill JR, Babayev Y, et al. (2009) Metastatic renal cell carcinoma risk according to tumor size. *J Urol* 182: 41–45
 26. Kunkle DA, Egleston BL, Uzzo RG (2008) Excise, ablate or observe: the small renal mass dilemma—a meta-analysis and review. *J Urol* 179:1227–1233
 27. Chawla SN, Crispen PL, Hanlon AL, et al. (2006) The natural history of observed enhancing renal masses: meta-analysis and review of the world literature. *J Urol* 175:425–431
 28. Smaldone MC, Kutikov A, Egleston BL, et al. (2012) Small renal masses progressing to metastases under active surveillance: a systematic review and pooled analysis. *Cancer* 118:997–1006
 29. Mason RJ, Abdolell M, Trottier G, et al. (2011) Growth kinetics of renal masses: analysis of a prospective cohort of patients undergoing active surveillance. *Eur Urol* 59:863–867
 30. Kouba E, Smith A, McRackan D, et al. (2007) Watchful waiting for solid renal masses: insight into the natural history and results of delayed intervention. *J Urol* 177:466–470
 31. Pierorazio PM, Hyams ES, Mullins JK, Allaf ME (2012) Active surveillance for small renal masses. *Nat Rev Urol* 14(1–2):13–19
 32. Volpe A, Kachura JR, Geddie WR, et al. (2007) Techniques, safety and accuracy of sampling of renal tumors by fine needle aspiration and core biopsy. *J Urol* 178:379
 33. Kümmerlin I, ten Kate F, Smedts F, et al. (2008) Core biopsies of renal tumors: a study on diagnostic accuracy, interobserver, and intraobserver variability. *Eur Urol* 53:1219
 34. Le Bret T, Poulain JE, Molin V, et al. (2007) Percutaneous core biopsy for renal masses: indications, accuracy and results. *J Urol* 178(4 Pt 1):1184
 35. Schmidbauer J, Remzi M, Memarsadeghi M, et al. (2008) Diagnostic accuracy of computed tomography-guided percutaneous biopsy of renal masses. *Eur Urol* 53:1003
 36. Jeon HG, Seo SI, Jeong BC, et al. (2015) Percutaneous kidney biopsy for a small renal mass: a critical appraisal of results. *J Urol* S0022–5347(15):4881–4888
 37. Chandarana H, Rosenkrantz AB, Mussi TC, et al. (2012) Histogram analysis of whole-lesion enhancement in differentiating clear cell from papillary subtype of renal cell cancer. *Radiology* 265:790–798
 38. Chen F, Huhdanpaa H, Desai B, et al. (2015) Whole lesion quantitative CT evaluation of renal cell carcinoma: differentiation of clear cell from papillary renal cell carcinoma. *Springerplus* 4:66
 39. Kim JY, Kim JK, Kim N, Cho KS (2008) CT histogram analysis: differentiation of angiomyolipoma without visible fat from renal cell carcinoma at CT imaging. *Radiology* 246(2):472–479